Brazilian Journal of Biology®

ISSN 1519-6984 (Print)
ISSN 1678-4375 (Online)

Original Article

Morpho-anatomical characterization and DNA barcoding of *Artemesia vulgaris* L.

Caracterização morfoanatômica e código de barras do DNA de *Artemesia vulgaris* L.

D. K. Wahyuni[a*], D. T. Indriati[a], M. Ilham[a], A. A. A. Murtadlo[a], H. Purnobasuki[a], Junairiah[a], P. R. Purnama[b], N. K. K. Ikram[c,d], M. Z. Samian[c,d] and S. Subramaniam[a,e]

[a] Universitas Airlangga, Faculty of Science and Technology, Department of Biology, Surabaya, East Java, Indonesia
[b] Chulalongkorn University, Faculty of Science, Graduate Program in Bioinformatics and Computational Biology, Bangkok, Thailand
[c] Universiti Malaya, Faculty of Science, Institute of Biological Sciences, Kuala Lumpur, Malaysia
[d] Universiti Malaya, Centre for Research in Biotechnology for Agriculture – CEBAR, Kuala Lumpur, Malaysia
[e] Universiti Sains Malaysia, School of Biological Science, Georgetown, Malaysia

Abstract

Artemisia vulgaris L. belongs to Asteraceae, is a herbal plant that has various benefits in the medical field, so that its use in the medical field can be explored optimally, the plant must be thoroughly identified. This study aims to identify *A. vulgaris* both in terms of descriptive morpho-anatomy and DNA barcoding using BLAST and phylogenetic tree reconstruction. The morpho-anatomical character was observed on root, stem, and leaf. DNA barcoding analysis was carried out through amplification and alignment of the *rbcL* and *matK* genes. All studies were conducted on three samples from Taman Husada (Medicinal Plant Garden) Graha Famili Surabaya, Indonesia. The anatomical slide was prepared by the paraffin method. Morphological studies revealed that the leaves of *A. vulgaris* both on the lower-middle part and on the upper part of the stem have differences, especially in the character of the stipules, petioles, and incisions they have. Meanwhile, from the study of anatomy, *A. vulgaris* has an anomocytic type of stomata and its distribution is mostly on the ventral part of the leaves. Through the BLAST process and phylogenetic tree reconstruction, the plant sequences being studied are closely related to several species of the genus *Artemisia* as indicated by a percentage identity above 98% and branch proximity between taxa in the reconstructed phylogenetic tree.

Keywords: *Artemisia vulgaris*, DNA barcode, morpho-anatomy, *matK*, phylogenetic tree, *rbcL*.

Resumo

Artemisia vulgaris L., pertencente à família Asteraceae, é uma planta herbácea com diversos benefícios à área médica. E para que seu uso na área médica possa ser explorado de forma otimizada, a planta deve ser minuciosamente identificada. Este estudo tem como objetivo identificar *A. vulgaris* por meio de análise morfoanatomia descritiva, quanto de código de barras do DNA utilizando BLAST e reconstrução de árvore filogenética. As características morfoanatômica foram observadas na raiz, caule e folha. A análise do código de barras do DNA foi realizada através da amplificação e alinhamento dos genes rbcL e matK. Todos os estudos foram feitos em três amostras de Taman Husada (Jardim de Plantas Medicinais) Graha Famili, Surabaya, Indonésia. A lâmina anatômica foi preparada pelo método da parafina. Estudos morfológicos revelaram que as folhas de *A. vulgaris*, tanto na parte média inferior quanto na parte superior do caule, apresentam diferenças, principalmente nos caracteres das estípulas, pecíolos e incisões. Já o estudo da anatomia revelou que *A. vulgaris* possui estômatos do tipo anomocítico e sua distribuição é principalmente na parte ventral das folhas. Através do processo BLAST e da reconstrução da árvore filogenética, as sequências de plantas em estudo apresentam estreira relação com várias espécies do gênero *Artemisia*, conforme indicado por uma identidade percentual acima de 98% e proximidade de ramos entre táxons na árvore filogenética reconstruída.

Palavras-chave: *Artemisia vulgaris*, código de barras de DNA, morfoanatomia, *matK*, árvore filogenética, *rbcL*.

1. Introduction

Artemisia vulgaris L. is a member of the genus *Artemisia* which belongs to the Asteraceae family, this family has significant economic and medical value. *A. vulgaris* has an important record in the history of medicine and is known as the "mother of herbs" in the Middle Ages (Ekiert et al., 2020). This plant is commonly used in traditional medicine practices, because of its therapeutic benefits, especially in urology (Zubair et al., 2020). Phytochemical studies of *A. vulgaris* resulted in the isolation of sterols, triterpenes, and flavonoids (Farrag et al., 2015). According to Barney and

*e-mail: dwi-k-w@fst.unair.ac.id
Received: September 11, 2023 – Accepted: January 6, 2024

Ditommaso (2003), *A. vulgaris* displays morphological and physiological heterogeneity at extreme levels in various ecologies, including branch properties, branching degree, leaf morphology, and rhizome diameter (Barney and Ditommaso, 2003). Therefore, in addition to identifying morpho-anatomically to prevent misrecognition, identification at the molecular level such as DNA barcoding is also required. Apart from the morphological diversity, molecular identification is required to confirm the identity of the plant before the plant undergoes further extractions and the extracts are used as ingredients in herbal or pharmaceutical products.

In general, species of the genus *Artemisia* are found in temperate regions, especially in the northern hemisphere and with limited numbers in the southern hemisphere (Oberprieler et al., 2009). This genus has many morphological and phytochemical characteristics, both of which are associated with the geographical origin of the plant habitat (Abuhadra et al., 2017). For example, various studies on the plant trichomes indicate the content of secondary metabolites stored by trichomes. Several Asteraceae species have trichomes containing terpenoids, alkaloids, phenols, and oils (Dorly et al., 2015). Mercado et al. (2021) reported that *Artemisia copa* has schizogenous secretory ducts distributed in the leaf midvein and cortex in the stem (Mercado et al., 2021). The use of anatomical markers alone will not be sufficient to produce maximum taxonomic data, because these markers also depend on environmental factors (Zagoto and Violita, 2019). To determine the content of secondary metabolites for pharmaceutical purposes, anatomical markers can also be used. A molecular approach, such as DNA barcoding develops into conclusive authentication and taxonomic assignment for phytopreparation quality assurance (Ulrich-Merzenich et al., 2007; Patwardhan et al., 2014).

DNA barcoding is a taxonomic method to identify DNA of organisms or a particular species (Sarvananda, 2018). DNA barcoding is a powerful and efficient tool for the identification of poorly studied species using short and standardized DNA fragments (Genievskaya et al., 2017; Kress, 2017; Ariyanti et al., 2021). There are 7 candidate DNA plastid markers, namely the *atpF-atpH, matK, rbcL, rpoB, rpoC1, psbK-psbI*, and *trnH-psbA*. However, based on various assessment criteria, the recommended DNA barcode for plants is a combination of *rbcL* and *matK* loci (CBOL Plant Working Group, 2009). One of the weaknesses of DNA barcodes is the non-universality of markers, therefore the selection of DNA barcode types in taxonomic studies is critical. Each taxa groups have its standard barcode. For example, in animals, the *mitochondrial cytochrome oxidase I (COI)* gene is generally used for phylogenetic study. However; the same gene cannot be employed in plants, as it lacks sufficient variations due to a low mutation rate (Ho et al., 2021). To select universal barcodes for plants, various molecular markers have been identified, including cpDNA regions such as *matK* (*maturase-K*) and *rbcL* (*ribulose-biphosphate carboxylase large subunit*) (Hilu and Liang, 1997; CBOL Plant Working Group, 2009). These areas were selected for three reasons: universality, sequence quality, and discriminatory (CBOL Plant Working Group, 2009; Hollingsworth, 2011). There is a close correlation between plant identification activities to obtain chemical compounds for medical purposes. Hence, this study aims to identify *A. vulgaris* based on morpho-anatomic and DNA barcode markers to reveal a more in-depth medical potential of this plant. This investigation is expected to add important insights since *A. vulgaris* has become a commodity for herbal medicine and medicinal products.

2. Materials and Methods

2.1. Materials

Three individuals of adult *A. vulgaris* plant samples were taken in September 2019 at Taman Husada Graha Famili, Surabaya, East Java, Indonesia. The plant species identification was confirmed by comparison with the herbarium collection at the Purwodadi Botanical Garden, Indonesian Institute of Sciences, Pasuruan, Indonesia. Three voucher specimens (No. AV0101112021, No. AV0201112021, and No. AV0301112021) were deposited in Plant Systematic Laboratory, Department of Biology, Universitas Airlangga, Surabaya, Indonesia.

2.2. Morpho-anatomical characterization

The morphologically observed organs of *Artemisia vulgaris* were based on the research by El-Sahhar et al. (2010), which is limited to vegetative organs (root, stem, and leaves) (El-Sahhar et al., 2010). Anatomical analysis were based on plant organs (rhizomes, stem, and leaves) used by Janaćković et al. (2021), except for generative organs. Anatomical preparations were prepared using the paraffin method. Briefly, plant tissue were immersed into paraffin blocks to produce thin preparations (Ilham et al., 2022). Sample preparation using this method includes the following steps: cutting, fixation, aspiration, dehydration, dealcoholization, infiltration, embedding, trimming, staining, and mounting (Sari et al., 2016). The process of making anatomical preparations began with cutting the tissue with a thickness of 0.5-1 cm, then the pieces of plant tissue were fixed in a solution of FAA (Formalin, Glacial Acetic Acid, and 70% Alcohol) and simultaneously aspirated (Santos et al., 2016; Susetyarini et al., 2020). The fixation stage is the most important part of histology and cytology techniques because it prevents protein denaturation (Jamie, 2010). Dehydration is a process to remove all the fluid contained in the tissue (Rina, 2013). Dehydration process was carried out using graded alcohol (50%, 70%, 95%, and 100%) and dealcoholization using clearing agents such as xylol (Santos et al., 2016; Susetyarini et al., 2020). Clearing using xylol is useful for removing alcohol from the tissue and replacing it with a certain solution (Waheed, 2012). Then, the purification medium was replaced using paraffin (as a planting medium) that previously had thawed with an incubator. Plant tissue was embedded into paraffin blocks to solidifies, then the paraffin block will be carved into a trapezium and will be cut to produce a thin ban using microtome (Santos et al., 2016; Susetyarini et al., 2020). According to Rina (2013), embedding of paraffin is done three times in a certain period of time. Paraffin band was attached to a glass object that had coated with albumin. The last procedure was to color a thin paraffin band with safranin and fast green compounds, then cover it at second time with a cover glass (Santos et al., 2016; Susetyarini et al., 2020). Anatomical preparations will be observed under a light microscope to observe the tissues with magnificent 200-400 ×. All chemical materials were produced by Merck (Germany) for analytical analysis. Morpho-anatomical data were taken once for representative characters.

2.3. DNA barcoding

2.3.1. DNA extraction

DNA extraction was performed using the Tiangen Plant Genomic Kit (Tiangen, Kit). The DNA was extracted from three individuals young leaves of *Artemisia vulgaris* and each replicate has a mass of 0.1 g. The concentration and purity of DNA was measured using a Thermo Scientific Multiskan Go with absorbances of λ 260 nm and λ 280 nm.

2.4. PCR amplification and sequencing

DNA amplification using 2 cpDNA primers, *rbcL* (Forward: 5'-AAG TTC CTC CAC CGA ACT GTA-3'; Reverse: 5'-TAC TGC GGG TAC ATG CAA G-3') and *matK* (Forward: 5'- TGG TTC AGG CTC TTC GCT ATT G-3'; Reverse: 5'-CTG ATA AAT CGG CCC AAA TCG C-3'). These two primers had previously used on *Soncus arvensis* (Wahyuni et al., 2019), *Achillea millefolium* (Ilham et al., 2022), *Pluchea indica* (Wahyuni et al., 2022), and *Cosmos caudatus* (Purnobasuki et al., 2022). These primers had been specially designed for the Asteraceae family, so that the primers attachment to the target gene has a high chance. The PCR reaction mixture was 35 µL containing: 7.5 µL GoTaq®Green Master Mix; both *rbcL* and *matK* primers with the volume of forward and reverse primers is 1.5 µL (concentration 350-500 nM), 5 µL of DNA template (50 ng-1) and nuclease-free water was added until the volume reached 35 µL. Amplification using PCR was carried out by setting it into 5 stages with different temperatures and times: predenaturation 95°C for 5 minutes which occurred for 1 cycle; 35 cycles for denaturation 94°C for 30 seconds, annealing 56°C for 45 seconds, extension 72 °C for 45 seconds; and one cycle for final extension 72°C for 5 minutes. Determination of the PCR product and DNA quality was using gel electrophoresis with 1% agarose gel (Murtiyaningsih, 2017) and visualized with a UV transluminator. Subsequently, the PCR product were sent for sequencing at 1st Base Sequencing Service (Axil Scientific Pte.Ltd., Singapore).

2.5. Data analysis

The data from the morpho-anatomical analysis were analyzed descriptively, while the DNA sequenced from the 1st Base Sequencing Service was further processed using Bioedit 7.4 and Mega X software. Geneious 2021.3.4 software was also used to determine the percentage of nitrogen base composition (Purnobasuki et al., 2022). Furthermore, the consensus data was used for the DNA alignment or matching stage through the online software BLAST (Basic Local Alignment Search Tool). In the final stage, the sample plant sequence data and sequence data from the GenBank database were subjected to phylogenetic tree reconstruction using Neighbor-Joining Method. The data used to form the phylogenetic trees were derived from DNA sequences of the 3 replications of *A. vulgaris* and 15 plant DNA sequences from the GenBank database that were closely related to the sample plants. Table 1 shows a list of 15 plants from the GenBank database with additional information.

Table 1. Plant data downloaded from GenBank.

Plant (*rbcL*)	Acession Number	Plant (*matK*)	Accesion number
Artemisia sieversiana	MG951499.1	*Artemisia vulgaris*	KR231888.1
Artemisia selengensis	MG951498.1	*Artemisia argyi*	KM386991.1
Artemisia selengensis	MG951497.1	*Artemisia montana*	KF887960.1
Artemisia nakaii	MG951494.1	*Artemisia sp.*	KF697692.1
Artemisia japonica	MG951491.1	*Artemisia montana*	LC635379.1
Artemisia hallaisanensis	MG951490.1	*Artemisia stolonifera*	NC_049572.1
Artemisia gmelinii	MG951489.1	*Artemisia vulgaris*	KX581939.1
Artemisia fukudo	MG951488.1	*Artemisia vulgaris*	KX581938.1
Artemisia freyniana	MG951487.1	*Artemisia vulgaris*	KX581937.1
Artemisia capillaris	MG951485.1	*Artemisia vulgaris*	KX581936.1
Chrysanthemum x morifolium	MK986830.1	*Chrysanthemum x morifolium*	MK986830.1
Chrysanthemum boreale	MN913565.1	*Chrysanthemum*	KX522942.1
Chrysanthemum lucidum	NC_040920.1	*Chrysanthemum*	KX783651.1
Chrysanthemum lucidum	MH028788.1	*Ajania fruticulosa*	KX526529.1
Chrysanthemum	KX522942.1	*Chrysanthemum indicum*	MW633069.1

3. Result

The results of descriptive morpho-anatomical observations and processing of DNA sequence data from sample plants and Asteraceae plants are shown in the figures and tables below.

3.1. Morpho-anatomical characterization

The morphology of the vegetative organs including root, stem, and leaves are shown in Figure 1. The general anatomy of the vegetative organs are shown in Figures 2 and 3. Meanwhile, the appearance of the accessory organs of the

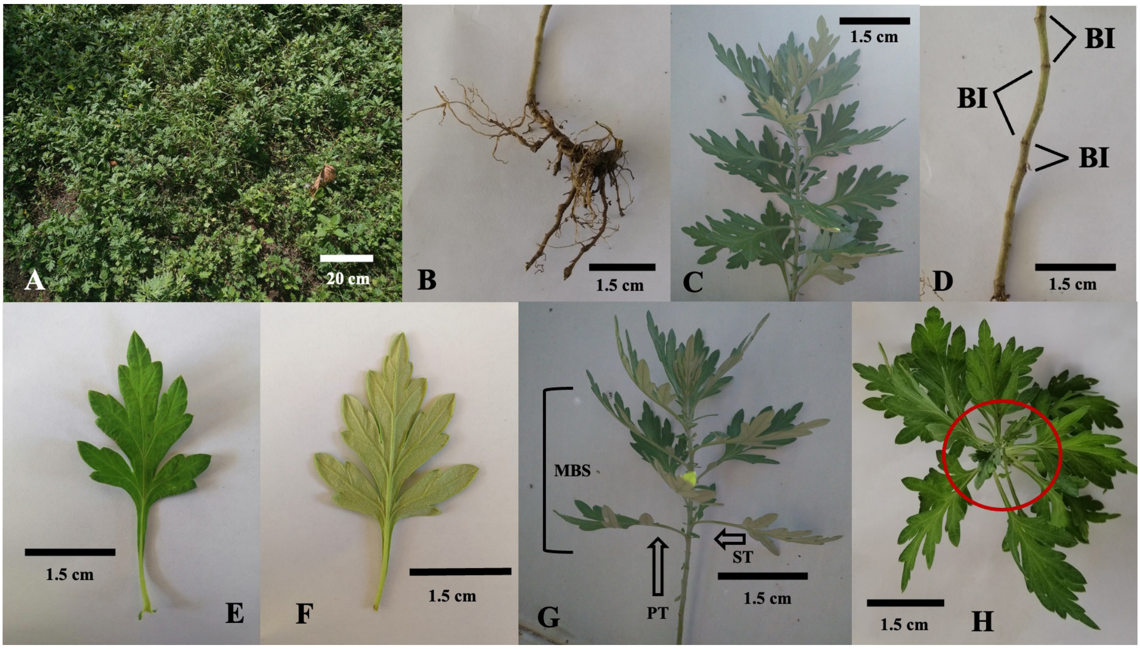

Figure 1. The morphology of the vegetative organs of Artemisia vulgaris: A. Habitus, B. Root, C. Stem and leaves, D. Distribution of internodes at the base of the stem (BI: basal internodes), E. Adaxial side, F. Abaxial side, G. Distribution of leaves on the middle-bottom of the stem (MBS: distribution of leaves in the middle-bottom of the stem, PT: petiole, and ST: stipule), H. Distribution of leaves on the top of the stem (marked with a red circle).

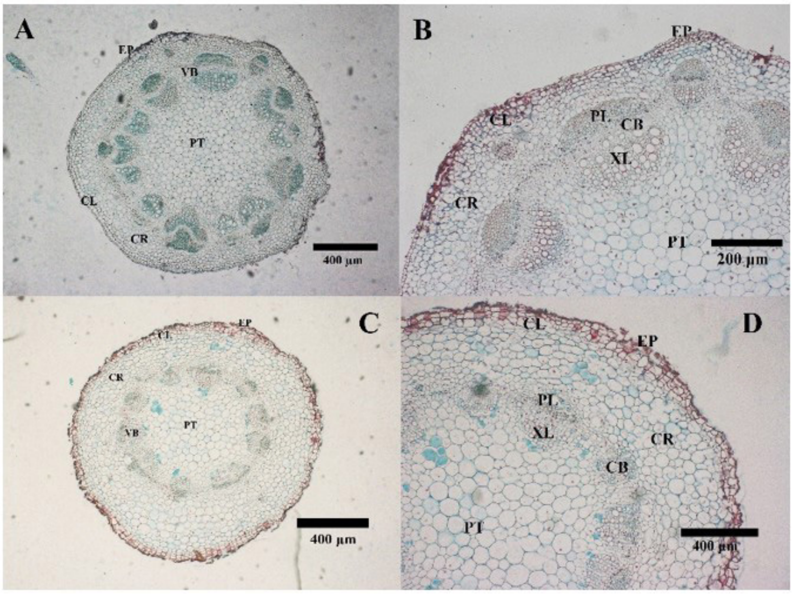

Figure 2. Anatomy of A-B. Stem and C-D. Rhizomes. EP: epidermis, CL: collenchyma, CR: cortex, VB: vascular bundles, PT: pith, PL: phloem, CB: cambium, and XL: xylem.

epidermis including trichomes and stomata are shown in Figure 4.

3.2. DNA barcoding

Quantitative measurement results of *Artemisia vulgaris* DNA are shown in Table 2 while qualitative measurement results are shown in Figure 5. Results of DNA processing in the form of nitrogen base percentages in Table 3, results of alignment using the BLAST NCBI program in Table 4, results of alignment with plants of close and distant relatives in Figure 6, and the phylogenetic trees in Figure 7.

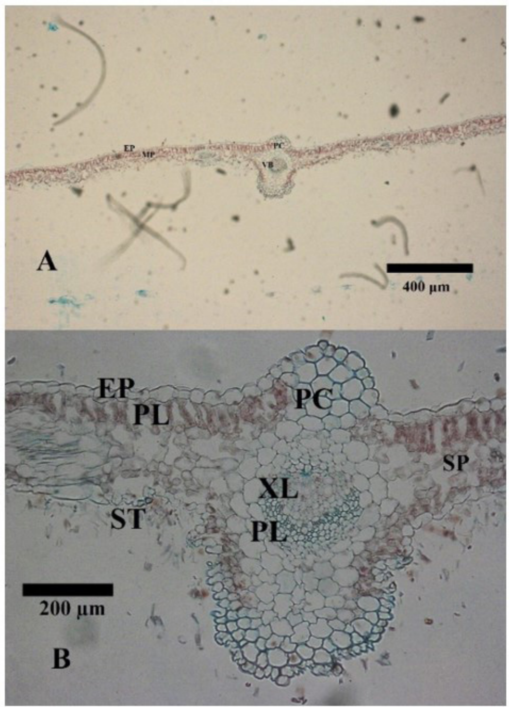

Figure 3. A-B. Anatomy of leaves *Artemisia vulgaris*. ST: Stomata. EP: epidermis, PC: parenchymal cortex, MP: Mesophyll, VB: vascular bundles, PL: palisade, SP: sponge, XL: xylem, and PL: phloem.

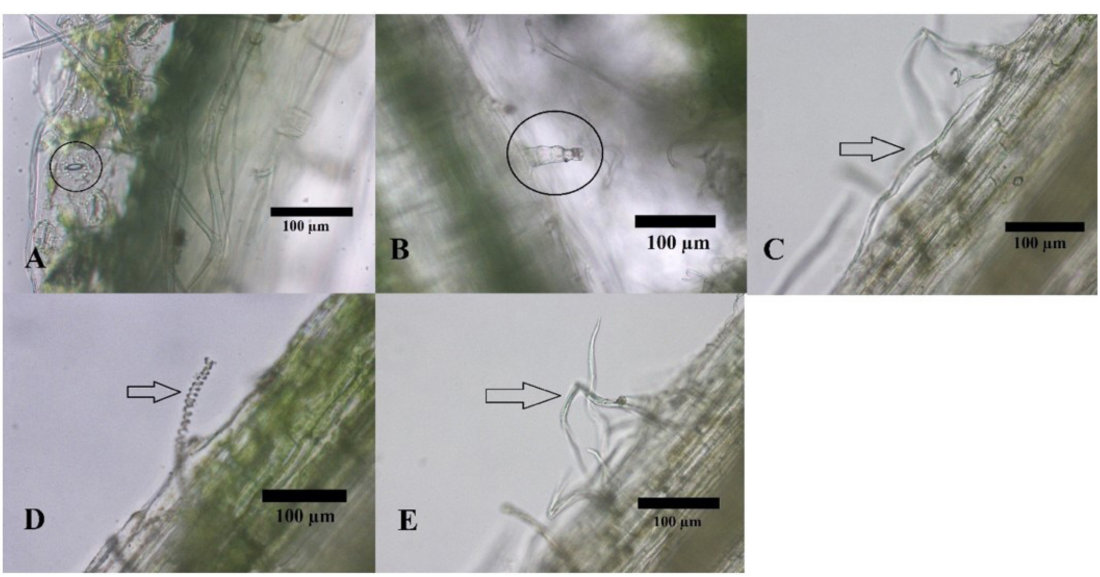

Figures 4. Anatomy of stomata and trichomes of *Artemisia vulgaris*: A. Stomata, B. Glandular trichomes, C. T-shaped trichomes, D. Spiral trichomes, E. Dragger- shaped trichomes.

3.2.1. Measurement of DNA purity and concentration

Table 2. Results of measurement of DNA purity and concentration.

Sample Name	Absorbance 1 (260 nm)	Absorbance 2 (280 nm)	Purity	Concentration (µg/µl)
Artemisia vulgaris 1	0.127	0.064	1.51	3.15
Artemisia vulgaris 2	0.103	0.071	1.45	1.95
Artemisia vulgaris 3	0.116	0.061	1.43	2.6

3.2.2. Visualization of electrophoresis results

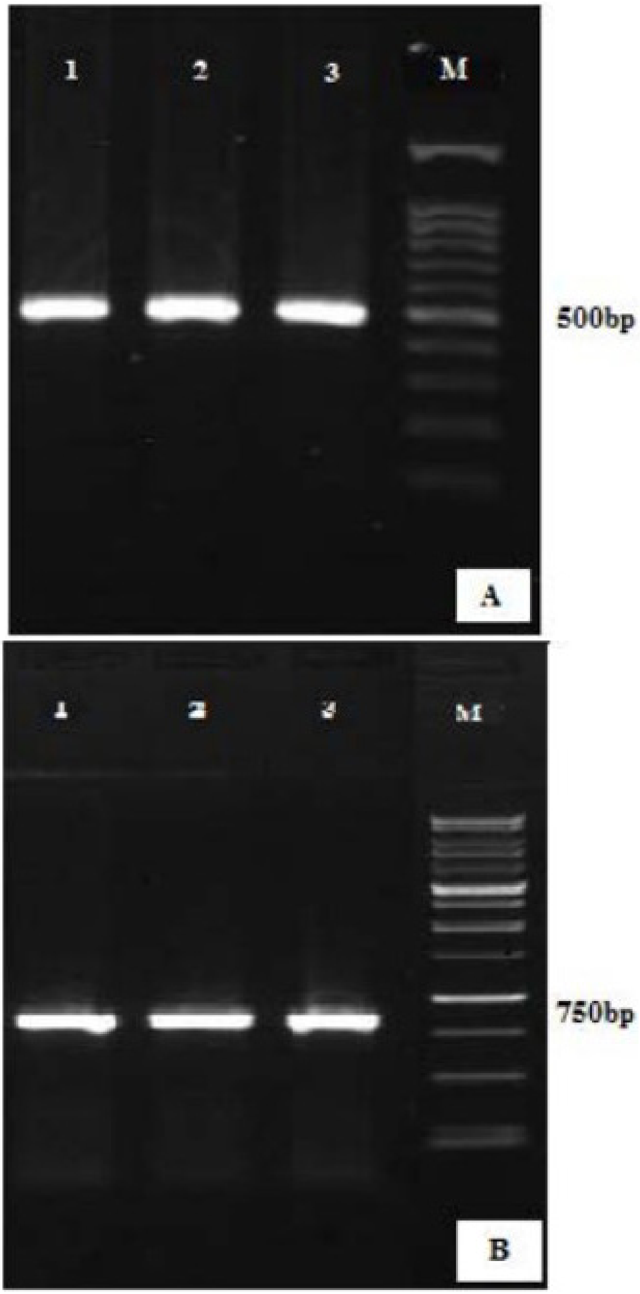

Figure 5. Amplification results of A. *rbcL* gene and B. *matK* gene.

3.2.3. DNA sequence analysis

Table 3. Comparison of the number of nitrogenous bases in *Artemisia vulgaris*.

Plant	Percentage of nitrogen bases
Artemisia vulgaris rbcL 1	A: 29.4%, C: 25.9%, G: 19.2%, T: 25.5%
Artemisia vulgaris rbcL 2	A: 30.0%, C: 25.7%, G: 18.8%, T: 25.5%
Artemisia vulgaris rbcL 3	A: 29.9%, C: 25.7%, G: 19.0%, T: 25.5%
Artemisia vulgaris matK 1	A: 29.1%, C: 18.2%, G: 15.9%, T: 36.8%
Artemisia vulgaris matK 2	A: 28.6%, C: 18.1%, G: 16.9%, T: 36.4%
Artemisia vulgaris matK 3	A: 28.5%, C: 18.2%, G: 16.9%, T: 36.4%

3.2.4. Alignment with sequences registered in GenBank

Table 4. Summary of alignment results of *rbcL* using BLAST.

rbcL						
Plant	**Max. Score**	**Total Score**	**Query Cover**	**E-Value**	**Percentage Identity**	**Accession Number**
Artemisia sieversiana	900	900	100%	0.0	99.80%	MG951499.1
Artemisia selengensis	900	900	100%	0.0	99.80%	MG951498.1
Artemisia selengensis	900	900	100%	0.0	99.80%	MG951497.1
Artemisia nakaii	900	900	100%	0.0	99.80%	MG951494.1
Artemisia japonica	900	900	100%	0.0	99.80%	MG951491.1
Artemisia hallaisanensis	900	900	100%	0.0	99.80%	MG951490.1
Artemisia gmelinii	900	900	100%	0.0	99.80%	MG951489.1
Artemisia fukudo	900	900	100%	0.0	99.80%	MG951488.1
Artemisia freyniana	900	900	100%	0.0	99.80%	MG951487.1
Artemisia capillaris	900	900	100%	0.0	99.80%	MG951485.1
Chrysanthemum x morifolium	894	894	100%	0.0	99.59%	MK986830.1
Chrysanthemum boreale	894	894	100%	0.0	99.59%	MN913565.1
Chrysanthemum lucidum	894	894	100%	0.0	99.59%	NC_040920.1
Chrysanthemum lucidum	894	894	100%	0.0	99.59%	MH028788.1
Chrysanthemum x morifolium	894	894	100%	0.0	99.59%	KX522942.1
matK						
Plant	**Max. Score**	**Total Score**	**Query Cover**	**E-Value**	**Percentage Identity**	**Accession Number**
Artemisia vulgaris	1279	1279	99%	0.0	99.86%	KR231888.1
Artemisia argyi	1279	1279	99%	0.0	99.86%	KM386991.1
Artemisia montana	1279	1279	99%	0.0	99.86%	KF887960.1
Artemisia sp.	1279	1279	99%	0.0	99.86%	KF697692.1
Artemisia montana	1279	1279	99%	0.0	99.86%	LC635379.1
Artemisia stolonifera	1279	1279	99%	0.0	99.86%	NC_049572.1
Artemisia vulgaris	1279	1279	99%	0.0	99.86%	KX581939.1
Artemisia vulgaris	1279	1279	99%	0.0	99.86%	KX581938.1
Artemisia vulgaris	1279	1279	99%	0.0	99.86%	KX581937.1
Artemisia vulgaris	1279	1279	99%	0.0	99.86%	KX581936.1
Chrysanthemum x morifolium	1232	1232	99%	0.0	99.84%	MK986830.1
Chrysanthemum x morifolium	1232	1232	99%	0.0	99.84%	KX522942.1
Chrysanthemum x morifolium	1232	1232	99%	0.0	99.84%	KX783651.1
Ajania fruticulosa	1232	1232	99%	0.0	99.84%	KX526529.1
Chrysanthemum indicum	1232	1232	99%	0.0	99.84%	MW633069.1

Figure 6. Comparison of the studied *Artemisa vulgaris* gene sequences with plants from the GenBank database. A. *rbcL*, B. *matK*. AV: *Artemisia vulgaris* being studied, AS: *Artemisia sieversiana* accession MG951499.1, CXM: *Chrysanthemum x morifolium* accession KX522942.1, AVG: *A. vulgaris* accession KR231888.1, CI: *Chrysanthemum indicum* accession MW633069.1. Blue circles indicate differences in nitrogenous bases and red circles indicate gaps.

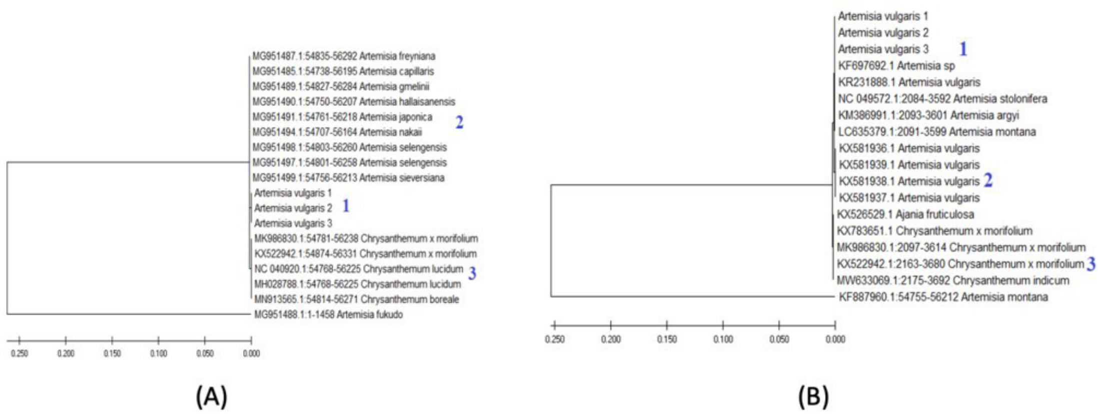

Figure 7. Phylogenetic tree of A. *rbcL*, B. *matK*.

4. Discussion

4.1. Morpho-anatomy characterization

Artemisia vulgaris has a shrub habitus, rarely seen in the form of perennial herbs, annual herbs or biennial herbs, this shrub habitus is common in most plants of the *Artemisia* genus (Abuhadra et al., 2017) (Figure 1A). *A. vulgaris* is a very common plant growing on nitrogenous soils, like weedy and uncultivated areas, such as waste places and roadsides (Setyawati et al., 2015). The plant has woody and brown root (Figure 1B) (Adams et al., 2012; Setiawati et al., 2008). The plant from the genus *Artemisia* has an erect stem, semiwoody, and the upper third of the stem is branched (Figure 1C). In terms of internodes, it generally has basal internode at the main stem, while in other areas of the stem, the internode is too short and surrounded by lush foliage (El-Sahhar et al., 2010) (Figure 1D). The young stem is terete and pubescent and older stem is somewhat purplish (Farrag et al., 2015; Wiart, 2003). The leaves of *A. vulgaris* are arranged densely and alternately, the position of the leaves are more inclined to the top of the stem (Figure 1C). The upper part of the lamina (dorsal) is dark green while the lower part (ventral) is light green (Barney and Ditommaso, 2003) (Figure 1E and 1F). Abaxial leaves also have tomentose hairs (Hayat et al., 2009b; Setyawati et al., 2015). This plant species has leaf with bifacial symmetry (Noorbakhsh et al., 2008). Most leaves of *A. vulgaris* are simplex, petiolate and stipulate. Leaf blades that located in the middle and bottom of the stem have edges with very deep notches (have highly dissected margins), pinnately lobed and the lobes are broadly lanceolate in shape with entire margins and apex acute, these primary lobes are often shallowly cleft by one or more secondary lobes (Figure 1G). The leaves at the top of the stem are also simplex, sessile (without petioles), exstipulate, and smaller in size compared to the leaves at the bottom, which are lanceolate in shape and the edges are not incised (Figure 1H). The leaves have a distinctive aroma when crushed (Weston et al., 2005; Farrag et al., 2015) and spicy taste (Borzabad et al., 2010).

The stem anatomy of *A. vulgaris* is almost the same as *Artemisia absinthium var. absinthium* and *Artemisia absinthium var. calcigena* (Konowalik and Kreitschitz, 2012), which consists of epidermal, collenchyma, cortex, transport bundles, and pith tissues (Figure 2A and 2B). The outermost tissue of the stem is called the epidermis, which is composed of a compact and dense layer of cells with a square to rectangular shape. There are no protective hairs or only a small number of broken bases of trichomes on the epidermis were observed (Ivanescu et al., 2015). Beneath the epidermis, there is a supporting tissue of young stem, namely collenchyma. The difference between epidermis and the collenchyma is related to the size of the cells and the number of cell layers. The collenchyma cells of *A. vulgaris* were larger and consisted of more than one layer of cells. According to Leroux (2012), in stem and petioles, collenchyma typically occurs in a peripheral position and can be found immediately beneath the epidermis (Leroux, 2012). The cortex which is composed of circular parenchyma cells, was not the largest tissue that composes the stem. The vascular bundles in this plant are collateral type, arranged in different sizes and have alternately circle patterns. Each bundle has a well-defined fibrous cap abutting the phloem (El-Sahhar et al., 2011). The arrangement of the xylem vessels in this plant is similar to *Artemisa absinthium*, the vessels are arranged in radial rows, continuously or discontinuously (Ivanescu et al., 2015). The cambium can be differentiated and represented by the presence of 3-4 cell rows (Farrag et al., 2015). The largest tissue that composes the stem is the pith. This tissue is formed by large parenchyma cells and is in the central region. The anatomy of the *A. vulgaris* rhizome in this study is similar to *Artemisia umbelliformis* rhizome (Janaćković et al., 2021) (Figure 2C and 2D). The rhizome is also known as a modified stem. From the observation, the size of the rhizomes' cortex, is quite large when compared to the stem.

Histology of *A. vulgaris* leaves has the same structure with flowering plants, composing of epidermal, mesophyll, cortical parenchyma, and vascular tissue (Figure 3A and 3B). On the leaf lobe surface, a single-layered epidermis was observed on both sides of the leaf. On the frontal side, the leaf epidermis is composed of a single layer cells with irregular polygonal shapes. In some areas of the epidermis, there are several gaps indicating the presence of stomata. According to Noorbakhsh et al. (2008), the plant from genus *Artemisia* have stomata only on the abaxial or inferior side of the leaf, such as in *Artemisia absinthium* var. *absinthium* and var. calcigena (Noorbakhsh et al., 2008; Konowalik and Kreitschitz, 2012). Hussain et al. (2019) also reported that from 13 *Artemisia* species, the majority showed the presence of stomata on the abaxial side. However, according to El-Sahhar et al. (2011) and Farrag et al. (2015), *A. vulgaris* stomata are found on both sides of the leaf, but the most abundant is on the abaxial side. In *Artemisia fragrans*, the number of stomata on the adaxial side is larger than the abaxial side (Sadigova, 2022). In addition, the type of stomata of this plant is anomocytic (Hussain, 2020), similar to the stomata of *Artemisia china* (Ermayanti et al., 2004) (Figure 4A). In this type of stomata, the subsidiary cells are indiscernible from other epidermal cells (Karbalaei et al., 2021).

Besides stomata, 2 general types of trichomes, namely glandular trichomes and non-glandular trichomes were also present in the epidermis. Trichomes play an important role in plant taxonomy due to its variance in size, shape, morphology, cell number and composition (Schilmiller et al., 2008). Non-glandular trichomes helps to deter herbivores, disperse seeds, absorb water and so on. While glandular trichomes act as storage, and secretion of various types of plant secondary metabolites (Wu et al., 2012). Several secondary metabolites produced by glandular trichomes are utilized in pharmaceutical industry for health purposes (Liu et al., 2019). The anatomy of the glandular trichomes of *A. vulgaris* is similar to *Artemisia annua*. These trichomes are composed of two basal cells, two stalk cells and six secretory cells (Duke and Paul, 1993; Juliarni et al., 2007; Cui et al., 2020) (Figure 4B), which are similar to other plants in general (Feng et al., 2021). These six secretory cells are border to the secretory cavity and contribute to filling the apical subcuticular space with secondary metabolites (Anders et al., 2012). Glandular trichomes of *A. vulgaris* only have one shape, while non-glandular trichomes have several shapes, such as letter "T" shape, spiral and Dragger-shaped. T-shaped trichomes are composed of stalk and elongated cells (Soetaert et al., 2013) (Figure 4C). T-shaped trichomes not only found in the same species (Noorbakhsh et al., 2008), but also in other species such as *Artemisia roxburghiana, Artemisia dubia, Artemisia moorcroftiana, Artemisia tangutica, Artemisia biennis, Artemisia macrocephala, Artemisia Japonica, Artemisia amygdalina, Artemisia absinthium,* and *Artemisia sieversiana* (Hayat et al., 2009a). In some species, such as *Artemisia annua*, the T-shaped trichomes have the oddity of being able to synthesize the anti malarial drug Artemisinin (Judd et al., 2019). Spiral trichomes have a folding form along their entire length, being erect or appressed (Roudi et al., 2020) (Figure 4D). Whereas dragger-shaped hair is rarely present and consists of 1 to 4 short basal cells with a dragger-shaped apical end cell (Farrag et al., 2015) (Figure 4E). In complex and changeable environment, non-glandular trichomes on plant surface plays important role than glandular trichomes. The morphology and structure of non-glandular trichomes varies with plant species, so the characteristics of non-glandular trichomes are regarded as important characteristics for microscopic identification of plant medicinal materials (Cui et al., 2020). Unlike the plants studied having 1 form of glandular trichomes and 3 forms of non-glandular trichomes, other plants such as *Artemisia argyi* have 2 forms of glandular trichomes and 1 form of non-glandular trichomes (Cui et al., 2020).

Many traits can be identified from the epidermis. The compact arrangement of epidermal cells and presence of stomata and trichomes are the main features of *A. vulgaris* leaf epidermis (El-Sahhar et al., 2011). According to Dickison (2000), characteristics of the leaf epidermis play an important role in the identification of a species. These characters include the types of trichome glands, number of subsidiary cells, size of the guard cells, orientation and distribution of the stomata and sizes of the epidermal cells. The foliar epidermal cells of *Artemisia* are remarkable characters for the distinction of different species (Hayat et al., 2009a). The tissue after epidermis is the mesophyll tissue. Mesophyll of *A. vulgaris* differentiated into palisade and spongy tissue (Figure 3A and 3B). Half of the mesophyll thickness is occupied by palisade tissue. The palisade tissue is located on one side of the leaf namely the adaxial side (Juliarni et al., 2007; Noorbakhsh et al., 2008; Farrag et al., 2015). The palisade tissue cells are oval, tightly arranged in 1 row and discontinuous in the midrib[3]. The palisade cells contain red-brown colored content (Farrag et al., 2015). When compared with *Artemisia china*, the palisade tissue of *A. china* has a slightly rounded shape (Ermayanti et al., 2004). Sponge tissue is located on the abaxial side of the leaf, with irregularly shaped cells and very low intercellular density, causing large intercellular spaces. These intercellular spaces show aerenchyma (Farrag et al., 2015). The midrib is more prominent on the abaxial side, where it displays the parenchymal cortex and bundle vessels in a spheroidal shape (Noorbakhsh et al., 2008) (Figure 3A and 3B). The xylem is located at the top (El-Sahhar et al., 2011), characterized by the presence of large vessels arranged radially. The plants studied were cultivated plants, therefore they differed from wild plants in terms of leaf vascular tissue. In the wild plant, the vascular tissue consisted of one large central vascular bundle and a smaller one at each side, while the cultivated plant showed only one central vascular bundle (Farrag et al., 2015) (Figure 3A and 3B).

4.2. DNA barcoding

4.2.1. Measurement of DNA purity and concentration

The results of DNA purity and concentration using a spectrophotometer is shown in Table 2. The DNA purity of *Artemisia vulgaris* has a value of 1.43-1.51, while the concentration ranges from 1.95-3.15µg/µl. DNA purity is determined by comparing the wavelength absorbed by DNA (260 nm) and contaminants such as protein and phenol (280 nm). The formula is λ 260 nm/ λ 280 nm and good DNA purity values are 1.8-2.0 (Dewanata and Mushlih, 2021). If the comparison value of λ 260/λ 280 is less than 1.8, it indicates the presence of phenol or protein contaminants from the extraction process, whereas if the ratio is more than 2.0, the DNA contains RNA (Rizko et al., 2020). Contamination could be from incomplete lysis of cell components or due to the presence of phenol during the isolation process (Gross-Bellard et al., 1973).

4.2.2. Visualization of electrophoresis results

The primers used in the PCR process succeeded in amplifying the *rbcL* and *matK* genes in *Artemisia vulgaris*, indicated by a good intense DNA band (Figure 5A and 5B). The thickness of the *rbcL* and *matK* gene bands belonging to *A. vulgaris* has the same quantity as *Achillea millefolium* (Ilham et al., 2022) and *Cosmos caudatus* (Purnobasuki et al., 2022), because the primer used was same. According to the National Laboratory of Enteric Pathogens (1991) the key to the success of the PCR in diagnosis resides in its ability to amplify regions within a single molecule of DNA which may have etiologic significance (National Laboratory of Enteric Pathogens, 1991). There are several factors that influence the appearance of DNA during the PCR process: (1*) triphosphate deoxyribonucleotide* (dNTP), (2) primer design, (3) DNA template, (4) buffer composition, (5) number of cycles during PCR, 6) enzymes and (7) technical and nontechnical factorsy (Yuwono, 2007). Among the seven factors, primer design is the most important factors in determining the success of PCR. This is because the primer identifies the region of the DNA of interest. Primer design can be done based on a known DNA sequence or from a sequence related to the target protein (Triyani et al., 2016). From the results of sequencing by the 1st Base and processing using Bioedit 7.4 and Mega X, the *rbcL* gene had 490 bp, 494 bp, and 495 bp of nucleotides. Meanwhile, the *matK* gene were 666 bp, 697 bp, and 698 bp. Compared with studies using the same primers for *Achillea millefolium* by Ilham et al. (2022) and *Cosmos caudatus* by Purnobasuki et al. (2022), the number of nucleotides was almost similar, with *rbcL* gene, ranging from size 470 -500 bp while *matK* gene from 690-710 bp. Furthermore, *A. vulgaris* DNA sequences were subjected to BLAST (Basic Local Alignment Search Tool) process, to compare the sequences with other DNA sequences in BOLD (Barcode of Life Database) (BOLD, 2021) and GenBank NCBI (NCBI, 2021; Tindi et al., 2017).

4.2.3. DNA sequence analysis

DNA sequence analysis was performed to determine the percentage of each nitrogenous base that makes up a gene. The *rbcL* gene from the three replications of *Artemisia vulgaris* has a composition of 29.4-30.0% adenine, 18.8-19.2% guanine, 25.7-25.9% cytosine, and 25.5% thymine. Meanwhile, the *matK* gene consists of 28.5-29.1% adenine, 15.9-16.9% guanine, 18.1-18.2% cytosine, and 36.4-36.8% thymine (Table 3). From the results, adenine and thymine dominates the nucleotide composition of the two genes. Adenine-thymine dominance also occurs in other plants such as *Cosmos caudatus* (Purnobasuki et al., 2022), *Sonchus arvensis* (Wahyuni et al., 2019), Pinus (Sing et al., 2021), seagrass (Stevanus and Pharmawati, 2021), and *Andrographis paniculate* (Arif et al., 2019). High adenine-thymine content is found in chloroplast-based genes as well as mitochondria-based genes such as the COI gene with similar characteristics (Nugroho et al., 2017; Rahayu et al., 2019). The result is in line with Smith et al. (2011) that adenine and thymine comprise most of the mitochondrial and plastid genome sequences. The higher adenine-thymine content than the guanine-cytosine content is due to the high variability in nucleotide composition and the higher rate of nucleotide substitution in the amplified gene (Ismail et al., 2020).

4.2.4. Alignment with sequences registered in GenBank

The results of the sequences alignment using the BLAST program showed that *rbcL* and *matK* of *Artemisia vulgaris* from the Taman Husada Graha Famili Surabaya collection had a high similarity percentage (percentage identity) of more than 98% in both plants from the same genus or plants from different genus within the Asteraceae family (Table 4). According to Janda and Abbott (2007), if the percentage identity has a value of 100% or above 97%, it can be confirmed as the same species. The absence of *A. vulgaris* sequences from the GenBank database for the *rbcL* gene is probably due to the plant species has not been registered. Besides percentage identity, the similarity or closeness between plant species can also be determine using other parameters such as e-value, query cover, and score. E-value shows similarity between the studied *A. vulgaris* DNA sequences with plants registered in the GenBank database, if the value is close to or same as 0.0, the similarity is even higher (Sahaba et al., 2021). Query coverage is the percentage of the nucleotides length aligned with the existing database on BLAST (Fathiya et al., 2018). The homology level will be higher if the query coverage percentage value is also higher (Mukhopadhyay et al., 2018).

There were differences in the number of nitrogen bases and gaps when the studied plants were compared with other plants that were closely related and distantly related. In the case of the *rbcL* gene, comparisons were made with *Artemisia sieversiana* accession MG951499.1 and *Chrysanthemum x morifolium* accession KX522942.1, while the *matK* gene was compared with *A. vulgaris* accession KR231888.1 and *Chrysanthemum indicum* accession MW633069.1. The type of mutation that occurs is a point mutation. Comparison based on *rbcL* gene shows that the transversion occurs at nitrogen bases number 724, 816, and 1212, while the transition occurs at nitrogen base number 725 (Figure 6A). In addition, comparison based on *matK* gene also shows mutation with a more complex variety with transition, transversion, insertion and deletion activities. The transition occurs at nitrogen base number 339, transversion at 385 while insertion and deletion occur at 751,752, 753, 754, 755, 756, 757, 758, 759, and 1040. The three plant replicates studied had different positions of nitrogen bases and gaps that were 100% similar when compared to the plants from the GenBank database, indicating that the three replicates were indeed the same species. This is in accordance with the statement of Yang et al. (2018) that each individual has an SNP (Single Nucleotide Polymorphism) or commonly known as point mutation, and the same species will have SNP positions at the same range of base pairs. If the comparison between the sequences based on the *rbcL* gene is further analyzed, the difference in the composition of the nitrogen base between the studied plants and *Artemisia sieversiana* accession mg951499.1 has a small quantity if compared to the studied plants with *chrysanthemum* x *morifolium* Accession KX5222942.1 (Figure 6A). This is similar with the *matK* gene, the difference in nitrogen bases and the gaps between the plants under study with *A. vulgaris* accession KR231888.1 are smaller than plants under study with *Chrysanthemum indicum* accession MW633069.1. This indicates a close relationship between levels of taxon groups with more or fewer differences in nitrogenous bases.

Point mutation is a mutation that involve the replacement of one base pair of nucleotide (Julianti et al., 2015). Differences in nucleotide composition are generally caused by substitution events, substitution activities include transition and transversion (Huelsenbeck and Nielsen, 1999). Meanwhile, gaps in the DNA sequence are caused by insertion and deletion activities (Fan et al., 2007). According to Pandey et al. (2020), the barcoding gap is defined as the relation between the maximum intraspecific distances within each species, and the minimum interspecific distance with its nearest neighbor (Pandey et al., 2020). The consequences of point mutation are broadly divided into three. The first is a silent mutation or synonym mutation, which occurs when changes in the nitrogenous bases in the DNA sequence do not change the sequence of amino acids that make up the protein (Zheng et al., 2014). Next is a missense mutation, a change that causes the replacement of one amino acid with another in a protein-coding gene region (Cotton and Scriver, 1998). The last is nonsense mutation, which adds a premature stop signal that hinders any further translation of a protein-coding gene (Torella et al., 2020).

4.2.5. Phylogenetic tree

rbcL gene provides a good resolution in classifying species based on their taxonomic level (Figure 7A). The *rbcL* gene phylogenetic tree is split into 3 main clusters, except for *Artemisia fukudo* accession MG951488.1 which is not part of the three clusters. Cluster number one contains three replicated plants being studied with the same branch size, this indicates they are identical and came from the same parent or ancestor. According to Chen et al. (2015), *rbcL* is a gene sequence in the chloroplast genome that is derived directly from the parent. If there is a discovery of plant sequences based on the *rbcL* gene that has minimal variation and a highly conservative site, it can be concluded that these plants came from the same parent or the same ancestor. Cluster number two contains many different species in the genus *Artemisia* and the last cluster contains various species in the genus *Chrysanthemum*. It should be noted that *A. vulgaris* from the GenBank database is not yet available for the *rbcL* gene. This is not the case for *matK* gene because *A. vulgaris* data is already available in the GenBank database (Figure 7B). The phylogenetic tree is split into three main clusters, except for *Artemisia montana* accession KF887960.1. Unlike *rbcL* gene phylogenetic tree, *matK* gene phylogenetic tree offers resolution of placing the same species into different clusters. This is the case for *A. vulgaris*, which occupies clusters number one and two. The reason could be because *matK* has vast substitution rates in comparison to other chloroplast genes, and its gene sequence lies among the lowest conserved plastid genes (Zarei et al., 2020). However, in plants of different genus, there is no problem in separation for example genera *Chrysanthemum* and *Ajania* do not mix with plants from the genus *Artemisia*. Even so, the similarity between *rbcL* and *matK* based phylogenetic trees still position the three plant replications studied into the same group. This indicates that the same apomorphic/synapomorphic characters have been derived from the monophyletic characters in these samples forming a cluster (Pangestika et al., 2015). A similar case has been reported by Tallei and Kolondam (2015) that single locus of *matK* gene cannot be used to differentiate species in *Myristica*; it can only be used to differentiate the genus level within the Myristicaceae family. Ho et al. (2021) also reported that the discriminating abilities of the *matK* and *rbcL* genes in jewel orchid plants showed a different level of efficiency, the *rbcL* gene was considered to have better discriminating power than the *matK* gene alone or the *rbcL*+*matK* gene combination. According to Alasmari (2020) the separability of the *matK* gene to differentiate between species is not always reliable, because in their study, only 2 samples of the 4 sequences tested could be identified correctly at the species level. The ideal locus for DNA barcoding of plants remains debatable since some loci are efficient for some taxonomic groups and the species discrimination of these genes varies among plant species. Although the result of the *matK* gene phylogenetic tree is not sufficiently accurate to differentiate plants at species level, the *rbcL* gene-based data would help with this deficiency, this is in accordance with the study by Dong et al. (2012) that one DNA barcoding marker is not enough to obtain sufficiently accurate and specific identification results (Dong et al., 2012), so *matK* and *rbcL* must be used as dual DNA barcoding procedures (Alasmari, 2020).

In this study, it can be concluded that *A. vulgaris* has distinctive morphological characteristics on its leaves. The leaves distributed on the bottom-center are characterized by being large, petiolate, stipules, and having deep notches. While the leaves located at the top of the stem are smaller in size, do not have petioles and stipules and the incisions are not too deep or do not have incisions at all. The key feature that is used as an anatomical standard to distinguish *A. vulgaris* from other plants is the histology of the epidermis, because it retains various unique characteristics of the stomata and trichomes. Trichomes have 2 types, namely glandular with one shape and non-glandular with three shapes (T-shaped, spiral, and dragger). Through the BLAST process and phylogenetic tree reconstruction, the plant sequences being studied are closely related to several species of the genus *Artemisia* as indicated by a percentage identity of above 98% and the proximity of branches between taxa in the reconstructed phylogenetic.

5. Conclusion

In summary, *Artemisia vulgaris* exhibits a shrub-like appearance and is commonly found in nitrogen-rich uncultivated areas. Its distinct features include an upright stem, and densely arranged alternate leaves with varied sizes and shapes, emitting a unique aroma when crushed. Notably, the leaves possess different types of trichomes, influencing their taxonomy and secondary metabolite production. The stem anatomy consists of distinct tissues, including epidermis with anomocitic stomata, collenchyma, cortex, vascular bundles, and pith. Through DNA barcoding using the *rbcL* and *matK* genes, the study establishes the plant's close relationship with other Artemisia species within the Asteraceae family. This comprehensive exploration sheds light on both the physical and molecular characteristics of *Artemisia vulgaris*, contributing to its identification and classification in the plant realm.

Acknowledgements

The authors thank Plant Medicinal Garden "Taman Husada Graha Famili" Surabaya, East Java Indonesia for providing sample plants. This study was financially supported by Universitas Airlangga, Indonesia 2023 Fiscal Year, following The Decree of Rector of Universitas Airlangga Number: 1601/UN3.LPPM/PT.01.03/2023.

References

ABUHADRA, M.N., MAKHLOUF, M.H. and ESSOKNE, R.F., 2017. A new record *Artemisia vulgaris* L. (Asteraceae) for the flora of Libya. *American Journal of Life Science Researches*, vol. 5, no. 3, pp. 83-88. http://dx.doi.org/10.21859/ajlsr-05033.

ADAMS, J.D., GARCÍA, C. and GARG, G., 2012. Mugwort (*Artemisia vulgaris, Artemisia douglasiana, Artemisia argyi*) in the treatment of menopause, premenstrual syndrome, dysmenorrhea, and attention deficit hyperactivity disorder. *Chinese Medicine*, vol. 3, no. 3, pp. 116-123. http://dx.doi.org/10.4236/cm.2012.33019.

ALASMARI, A., 2020. DNA-barcoding of some medicinal plant species in Saudi Arabia using *rbcL* and *matK* genes. *Phyton*, vol. 89, no. 4, pp. 1059-1081. http://dx.doi.org/10.32604/phyton.2020.010952.

ANDERS, S., REYES, A. and HUBER, W., 2012. Detecting differential usage of exons from RNA-Seq data. *Genome Research*, vol. 22, no. 10, pp. 2008-2017. http://dx.doi.org/10.1101/gr.133744.111. PMid:22722343.

ARIYANTI, Y., RINI, I.A., OKTAVIANI, I. and LEKSIKOWATI, S.S., 2021. DNA barcoding for selected mangrove-based estuary fishes from Way Kambas National Park, Lampung Province, Indonesia. *Journal of Tropical Life Science*, vol. 11, no. 2, pp. 151-160. http://dx.doi.org/10.11594/jtls.11.02.04.

BARNEY, J.N. and DITOMMASO, A., 2003. The biology of Canadian weeds. (*Artemisia vulgaris* L.). *Canadian Journal of Plant Science*, vol. 83, no. 1, pp. 205-215. http://dx.doi.org/10.4141/P01-098.

BOLD, 2021 [viewed 10 June 2021]. *Barcode of life system* [online]. Available from: http://boldsystems.org.

BORZABAD, R.K., SUDARSHANA, M.S. and NIRANJAN, M.H., 2010. In vitro plant regeneration from leaf explants of *Artemisia vulgaris* L.–a medicinal herb. *Modern Applied Science*, vol. 4, no. 9, pp. 130-134. http://dx.doi.org/10.5539/mas.v4n9p130.

CBOL PLANT WORKING GROUP, 2009. A Barcode for land plants. *Proceedings of the National Academy of Sciences of the United States of America*, vol. 106, no. 31, pp. 12794-12797. http://dx.doi.org/10.1073/pnas.0905845106. PMid:19666622.

CHEN, Y., WANG, B., CHEN, J., WANG, X., WANG, R., PENG, S., CHEN, L., MA, L. and LUO, J., 2015. Identification of rubisco *rbcL* and *rbcS* in Camellia oleifera and their potential as molecular markers for selection of high tea oil cultivars. *Frontiers in Plant Science*, vol. 6, p. 189. http://dx.doi.org/10.3389/fpls.2015.00189. PMid:25873921.

COTTON, R.G.H. and SCRIVER, C.R., 1998. Proof of disease-causing mutation. *Human Mutation*, vol. 12, no. 1, pp. 1-3. http://dx.doi.org/10.1002/(SICI)1098-1004(1998)12:1<1::AID-HUMU1>3.0.CO;2-M. PMid:9633813.

CUI, Z., HUANG, X., LI, C., LI, Z., LI, M., GU, L., GAO, L., LIU, D. and ZHANG, Z., 2020. Morphology, distribution, density and chemical composition of glandular trichomes in *Artemisia argyi* (Asteraceae). *International Journal of Agriculture and Biology*, vol. 24, pp. 359-365. http://dx.doi.org/10.17957/IJAB/15.1445.

DEWANATA, P.A. and MUSHLIH, M., 2021. Differences in DNA purity test using UV-Vis spectrophotometer and nanodrop spectrophotometer in type 2 diabetes mellitus patients. *Indonesian Journal of Innovation Studies*, vol. 15, pp. 1-10. http://dx.doi.org/10.21070/ijins.v15i.553.

DICKISON, W.C., 2000. *Integrative plant anatomy*. San Diego: Academic Press.

DONG, W., LIU, J., YU, J., WANG, L. and ZHOU, S., 2012. Highly variable chloroplast markers for evaluating plant phylogeny at low taxonomic levels and for DNA barcoding. *PLoS One*, vol. 7, no. 4, p. e35071. http://dx.doi.org/10.1371/journal.pone.0035071. PMid:22511980.

DORLY, D., WIRYO, B.A., NURFAIZAH, I. and NIDYASARI, R.S., 2015. Secretory structure and histochemistry tests of Asteraceae family members of medicinal plants in Walat Mountain Educational

Forest. In: *Seminar Nasional XII Pendidikan Biologi FKIP UNS*, November 2015, Surakarta, Indonesia. Surakarta, Indonesia: Sebelas Maret University, vol. 2, no. 1, pp. 667-673.

DUKE, S.O. and PAUL, R.N., 1993. Development and fine structure of the glandular trichomes of *Artemisia annua* L. *International Journal of Plant Sciences*, vol. 154, no. 1, pp. 107-118. http://dx.doi.org/10.1086/297096.

EKIERT, H., PAJOR, J., KLIN, P., RZEPIELA, A., ŚLESAK, H. and SZOPA, A., 2020. Significance of *Artemisia vulgaris* L. (common mugwort) in the history of medicine and its possible contemporary applications substantiated by phytochemical and pharmacological studies. *Molecules*, vol. 25, no. 19, p. 4415. http://dx.doi.org/10.3390/molecules25194415. PMid:32992959.

EL-SAHHAR, K.F., NASSAR, R.M. and FARAG, H.M., 2010. Morphological and anatomical studies of *Artemisia vulgaris* L. (Asteraceae). I. Morphological characteristics. *Journal of American Science*, vol. 6, no. 9, pp. 806-814.

EL-SAHHAR, K.F., NASSAR, R.M. and FARAG, H.M., 2011. Morphological and anatomical studies of *Artemisia vulgaris* L. (Asteraceae) II. anatomical characteristics and volatile oil. *Australian Journal of Basic and Applied Sciences*, vol. 5, no. 6, pp. 56-68.

ERMAYANTI, T.M., JULIARNI, J. and ANDRY, Y., 2004. Leaf anatomical structure of *Artemisia cina* Berg. Ex Poljakov grown in tissue culture. *Biota*, vol. 9, no. 3, pp. 144-154. http://dx.doi.org/10.24002/biota.v9i3.2911.

FAN, Y., WANG, W., MA, G., LIANG, L., SHI, Q. and TAO, S., 2007. Patterns of insertion and deletion in mammalian genomes. *Current Genomics*, vol. 8, no. 6, pp. 370-378. http://dx.doi.org/10.2174/138920207783406479. PMid:19412437.

FARRAG, N.M., DAHLIA, I.H. and WAFAA, M.I., 2015. Macro- and micromorphological study of *Artemisia vulgaris* L. Fam. Asteraceae growing in Egypt. *Zagazig Journal of Pharmaceutical Science*, vol. 24, no. 2, pp. 109-134. http://dx.doi.org/10.21608/zjps.2015.38170.

FATHIYA, N., HARNELLY, E., THOMY, Z. and IQBAR, I., 2018. Molecular identification of *Shorea johorensis* in Ketambe Research Station, Gunung Leuser National Park. *Jurnal Natural*, vol. 18, no. 2, pp. 56-64. http://dx.doi.org/10.24815/jn.v18i2.10123.

FENG, Z., BARTHOLOMEW, E.S., LIU, Z., CUI, Y., DONG, Y., LI, S., WU, H., REN, H. and LIU, X., 2021. Glandular trichomes: new focus on horticultural crops. *Horticulture Research*, vol. 8, no. 1, p. 158. http://dx.doi.org/10.1038/s41438-021-00592-1. PMid:34193839.

GENIEVSKAYA, Y., ABUGALIEVA, S., ZHUBANYSHEVA, A. and TURUSPEKOV, Y., 2017. Morphological description and DNA barcoding study of sand rice (*Agriophyllum squarrosum*, Chenopodiaceae) collected in Kazakhstan. *BMC Plant Biology*, vol. 17, suppl. 1, p. 177. http://dx.doi.org/10.1186/s12870-017-1132-1. PMid:29143601.

GROSS-BELLARD, M., OUDET, P. and CHAMBON, P., 1973. Isolation of high molecular weight DNA from mammalian cells. *European Journal of Biochemistry*, vol. 36, no. 1, pp. 32-38. http://dx.doi.org/10.1111/j.1432-1033.1973.tb02881.x. PMid:4200179.

HAYAT, M.Q., ASHRAF, M., KHAN, M.A., YASMIN, G., SHAHEEN, N. and JABEEN, S., 2009a. Diversity of foliar trichomes and their systematic implications in the genus Artemisia (Asteraceae). *International Journal of Agriculture and Biology*, vol. 11, no. 5, pp. 542-546.

HAYAT, M.Q., KHAN, M.A., ASHRAF, M.A. and JABEEN, S.S., 2009b. Ethnobotany of the genus Artemisia (Asteraceae) in Pakistan. *Ethnobotany Research and Applications*, vol. 7, pp. 147-162. http://dx.doi.org/10.17348/era.7.0.147-162.

HILU, K.W. and LIANG, H.G., 1997. The matK gene: sequence variation and application in plant systematics. *American Journal of Botany*, vol. 84, no. 6, pp. 830-839. http://dx.doi.org/10.2307/2445819. PMid:21708635.

HO, V.T., TRAN, T.K.P., VU, T.T.T. and WIDIARSIH, S., 2021. Comparison of *matK* and *rbcL* DNA barcodes for genetic classification of jewel orchid accessions in Vietnam. *Journal of Genetic Engineering and Biotechnology*, vol. 19, no. 1, p. 93. http://dx.doi.org/10.1186/s43141-021-00188-1. PMid:34152504.

HOLLINGSWORTH, P.M., 2011. Refining the barcode for land plants. *Proceedings of the National Academy of Sciences of the United States of America*, vol. 108, no. 49, pp. 19451-19452. http://dx.doi.org/10.1073/pnas.1116812108. PMid:22109553.

HUELSENBECK, J.P. and NIELSEN, R., 1999. Variation in the pattern of nucleotide substitution across sites. *Journal of Molecular Evolution*, vol. 48, no. 1, pp. 86-93. http://dx.doi.org/10.1007/PL00006448. PMid:9873080.

HUSSAIN, A., 2020. The genus Artemisia (Asteraceae): a review on its ethnomedicinal prominence and taxonomy with emphasis on foliar anatomy, morphology, and molecular phylogeny. *Proceedings of the Pakistan Academy of Sciences: B. Life and Environmental Sciences*, vol. 57, no. 1, pp. 1-28.

HUSSAIN, A., HAYAT, M.Q., SAHREEN, S. and BOKHARI, S.A., 2019. Unveiling the foliar epidermal anatomical characteristics of genus Artemisia (Asteraceae) from northeast (Gilgit-Baltistan), Pakistan. *International Journal of Agriculture and Biology*, vol. 21, no. 3, pp. 630-638.

ILHAM, M., MUKARROMAH, S.R., RAKASHIWI, G.A., INDRIATI, D.I., YOKU, B.F., PURNAMA, P.R., JUNAIRIAH, J., PRASONGSUK, S., PURNOBASUKI, H. and WAHYUNI, D.K., 2022. Morpho-anatomical characterization and DNA barcoding of *Achillea millefolium* L. *Biodiversitas*, vol. 23, no. 4, pp. 1958-1969. http://dx.doi.org/10.13057/biodiv/d230430.

ISMAIL, M., AHMAD, A., NADEEM, M., JAVED, M.A., KHAN, S.H., KHAWAISH, I., STHANADAR, A.A., QARI, S.H., ALGHANEM, S.M., KHAN, K.A., KHAN, M.F. and QAMER, S., 2020. Development of DNA barcodes for selected Acacia species by using *rbcL* and *matK* DNA markers. *Saudi Journal of Biological Sciences*, vol. 27, no. 12, pp. 3735-3742. http://dx.doi.org/10.1016/j.sjbs.2020.08.020. PMid:33304185.

IVANESCU, B., ANCA, M. and CRISTINA, L., 2015. Histo-anatomy of vegetative organs of some Artemisia species. *Revista Medico-Chirurgicală*, vol. 119, no. 3, pp. 917-924.

JAMIE, M., 2010. *Education guide: special stains and H&E*. 2nd ed. California: Dako North America.

JANAĆKOVIĆ, P., GAVRILOVIĆ, M., RANČIĆ, D., STEŠEVIĆ, D., DAJIĆ-STEVANOVIĆ, Z. and MARIN, P.D., 2021. Anatomical traits of *Artemisia umbelliformis* subsp. eriantha (Asteraceae) alpine glacial relict from Mt. Durmitor (Montenegro). *Botanica Serbica*, vol. 45, no. 1, pp. 23-30. http://dx.doi.org/10.2298/BOTSERB2101023J.

JANDA, J.M. and ABBOTT, S.I., 2007. 16S rRNA gene sequencing for bacterial identification in the diagnostic laboratory pulses, perils, and pitfalls. *Journal of Clinical Microbiology*, vol. 45, no. 9, pp. 2761-2764. http://dx.doi.org/10.1128/JCM.01228-07. PMid:17626177.

JUDD, R., BAGLEY, M.C., LI, M., ZHU, Y., LEI, C., YUZUAK, S., EKELÖF, M., PU, G., ZHAO, X., MUDDIMAN, D.C. and XIE, D.Y., 2019. Artemisinin biosynthesis in non-glandular trichome cells of Artemisia annua. *Molecular Plant*, vol. 12, no. 5, pp. 704-714. http://dx.doi.org/10.1016/j.molp.2019.02.011. PMid:30851440.

JULIANTI, E., PINARIA, A., LENGKONG, E. and KOLONDAM, B., 2015. DNA barcoding daluga plant (*Cyrtosperma spp.*) of Sangihe Island based on matK gene. *Jurnal Bios Logos*, vol. 5, no. 2, pp. 46-54. http://dx.doi.org/10.35799/jbl.5.2.2015.10547.

JULIARNI, J., DEWANTO, H.A. and ERMAYANTI, T.M., 2007. Leaf anatomical characters from shoot culture of *Artemisia annua* L. *Indonesian Journal of Agronomy*, vol. 35, no. 3, pp. 225-232. http://dx.doi.org/10.24831/jai.v35i3.1336.

KARBALAEI, Z., ROOFIGAR, A.A., BALALI, G.R. and BAGHERI, A., 2021. Foliar micromorphology of some selected species of the genus Artemisia and its taxonomic implications. *Rostaniha*, vol. 22, no. 2, pp. 273-285. http://dx.doi.org/10.22092/BOTANY.2022.356460.1277.

KONOWALIK, K. and KREITSCHITZ, A., 2012. Morphological and anatomical characteristics of *Artemisia absinthium* var. absinthium and its Polish endemic variety *A. absinthium* var. calcigena. *Plant Systematics and Evolution*, vol. 298, no. 7, pp. 1325-1336. http://dx.doi.org/10.1007/s00606-012-0639-z.

KRESS, W.J., 2017. Plant DNA barcodes: applications today and in the future. *Journal of Systematics and Evolution*, vol. 55, no. 4, pp. 291-307. http://dx.doi.org/10.1111/jse.12254.

LEROUX, O., 2012. Collenchyma: a versatile mechanical tissue with dynamic cell walls. *Annals of Botany*, vol. 110, no. 6, pp. 1083-1098. http://dx.doi.org/10.1093/aob/mcs186. PMid:22933416.

LIU, Y., JING, S.X., LUO, S.H. and LI, S.H., 2019. Non-volatile natural products in plant glandular trichomes: chemistry, biological activities, and biosynthesis. *Natural Product Reports*, vol. 36, no. 4, pp. 626-665. http://dx.doi.org/10.1039/C8NP00077H. PMid:30468448.

MERCADO, M.I., MARCIAL, G., CATALÁN, J.V., GRAU, A., CATALÁN, C.A.N. and PONESSA, G.I., 2021. Morphoanatomy, histochemistry, essential oil, and other secondary metabolites of *Artemisia copa* (Asteraceae). *Botany Letters*, vol. 168, no. 4, pp. 577-593. http://dx.doi.org/10.1080/23818107.2021.1956585.

MUKHOPADHYAY, C.S., CHOUDHARY, R.K. and IQUEBAL, M.A., 2018. *Basic applied bioinformatics*. Hoboken: John Wiley & Sons.

MURTIYANINGSIH, H., 2017. DNA genom isolation and identification of genetic relationship pineapple using RAPD (random amplified polimorfic DNA). *Agritop*, vol. 15, no. 1, pp. 84-93.

NATIONAL CENTER FOR BIOTECHNOLOGY INFORMATION - NCBI, 2021 [viewed 10 June 2021]. *Basic Local Alignment Search Tool, National Center for Biotechnology Information* [online]. Available from https://blast.ncbi.nlm.nih.gov.

NATIONAL LABORATORY OF ENTERIC PATHOGENS, BUREAU OF MICROBIOLOGY, LABORATORY CENTRE FOR DISEASE CONTROL, 1991. The polymerase chain reaction: an overview and development of diagnostic PCR protocols at the LCDC. *The Canadian Journal of Infectious Diseases*, vol. 2, no. 2, pp. 89-91. http://dx.doi.org/10.1155/1991/580478. PMid:22529715.

NOORBAKHSH, S.N., GHAHREMAN, A. and ATTAR, F., 2008. Leaf anatomy of Artemisia (Asteraceae) in Iran and its taxonomic implications. *Iranian Journal of Botany*, vol. 14, no. 1, pp. 54-69.

NUGROHO, E.D., NAWIR, D., AMIN, M. and LESTARI, U., 2017. DNA barcoding of nomei fish (Synodontidae: *Harpadon sp*.) in Tarakan Island, Indonesia. *Aquaculture, Aquarium, Conservation & Legislation*, vol. 10, no. 6, pp. 1466-1474.

OBERPRIELER, C.H., HIMMELREICH, S., KÄLLERSJÖ, M., VALLÈS, J., WATSON, L.E. and VOGT, R., 2009. Tribe Anthemideae. In: V.A. FUNK, A. SUSANNA, T. STUESSY and R. BAYER, eds. *Systematics, evolution and biogeography of the Compositae*. Vienna: International Association for Plant Taxonomy, pp. 631-662.

PANDEY, P.K., SINGH, Y.S., TRIPATHY, P.S., KUMAR, R., ABUJAM, S.K. and PARHI, J., 2020. DNA barcoding and phylogenetics of freshwater fish fauna of Ranganadi River, Arunachal Pradesh. *Gene*, vol. 754, p. 144860. http://dx.doi.org/10.1016/j.gene.2020.144860. PMid:32531457.

PANGESTIKA, Y., BUDIHARJO, A. and KUSUMANINGRUM, H.P., 2015. Phylogenetic analysis of *Curcuma zedoaria* (temu putih) based on internally transcribed spacer (ITS) genes. *Jurnal Akademika Biologi*, vol. 4, no. 4, pp. 8-14.

PATWARDHAN, A., RAY, S. and ROY, A., 2014. Molecular markers in phylogenetic studies - a review. *Journal of Phylogenetics & Evolutionary Biology*, vol. 2, no. 2, p. 1000131. http://dx.doi.org/10.4172/2329-9002.1000131.

PURNOBASUKI, H., RAKHASHIWI, G.A., JUNAIRIAH, WAHYUNI, D.K., PUTRA, R.E., RAFFIUDIN, R. and SOESSILOHADI, R.H., 2022. Morpho-anatomical characterizationand DNA barcode of *Cosmos caudatus* Kunth. *Biodiversitas*, vol. 23, no. 8, pp. 4097-4108. http://dx.doi.org/10.13057/biodiv/d230830.

RAHAYU, D.A., NUGROHO, E.D. and LISTYORINI, D., 2019. DNA Barcoding ikan introduksi khas Telaga Sari, Kabupaten Pasuruan. *Biotropika: Journal of Tropical Biology*, vol. 7, no. 2, pp. 51-62. http://dx.doi.org/10.21776/ub.biotropika.2019.007.02.2.

RINA, S., 2013. *Microtechnical practical instructions*. Yogyakarta: FK UGM/Department of Histology and Cell Biology.

RIZKO, N., HERMIN, P.K., REJEKI, S.F., SRI, P. and TIA, E., 2020. DNA isolation of red pomelo leaves (*Citrus maxima* Merr.) with modification of the doyle and doyle method. *Berkala Bioteknologi*, vol. 3, no. 2, pp. 1-7.

ROUDI, E., KHODAYARI, H., MOZAFFARIAN, V. and ZARRE, S., 2020. Trichome micromorphology and its significance in the systematics of Convolvulus L. (Convolvulaceae). *Turkish Journal of Botany*, vol. 44, no. 2, pp. 178-191. http://dx.doi.org/10.3906/bot-1907-20.

SADIGOVA, N.I., 2022. Morphoanatomical features of *Artemisia fragrans* species. *International Journal of Botany Studies*, vol. 7, no. 8, pp. 44-48.

SAHABA, M.A.B., ABDULLAH, A. and NUGRAHA, R., 2021. DNA barcoding for fresh shark products authentication from West Nusa Tenggara Waters. *Jurnal Pengolahan Hasil Perikanan Indonesia*, vol. 24, no. 3, pp. 407-414. http://dx.doi.org/10.17844/jphpi.v24i3.38318.

SANTOS, R.F., NUNES, B.M., SÁ, R.D., SOARES, L.A.L. and RANDAU, K.P., 2016. Morpho-anatomical study of *Ageratum conyzoides. Revista Brasileira de Farmacognosia*, vol. 26, no. 6, pp. 679-687. http://dx.doi.org/10.1016/j.bjp.2016.07.002.

SARI, D.P., FATMAWATI, U. and PRABASARI, R.M., 2016. Profile of hands on activity in microtechnical courses. *Proceeding Biology Education Conference*, vol. 13, no. 1, pp. 476-481.

SARVANANDA, L., 2018. Short introduction of DNA barcoding. *International Journal of Research*, vol. 5, no. 4, pp. 673-686.

SCHILMILLER, A.L., LAST, R.L. and PICHERSKY, E., 2008. Harnessing plant trichome biochemistry for the production of useful compounds. *The Plant Journal*, vol. 54, no. 4, pp. 702-711. http://dx.doi.org/10.1111/j.1365-313X.2008.03432.x. PMid:18476873.

SETIAWATI, W., MURTANINGSIH, R., GUNAENI, N. and RUBIATI, T., 2008. *Plants botanical pesticides and methods of production for control of plant destruction organisms (OPT). Prima Tani Balitsa*. Bandung: Research Institute for Vegetable Plants/Center for Research and Development of Horticulture/Agricultural Research and Development Agency.

SETYAWATI, T., SARI, N., INDRA, P.B. and GILANG, T.R., 2015. *A guide book to invasive alien plant species in Indonesia*. Bogor: Research, Development and Innovation Agency/Ministry of Environment and Forestry.

SING, L., DIXIT, P., SRIVASTAVA, R.P., PANDEY, S., SINGH, A., VERMA, P.C. and SAXENA, G., 2021. Phylogenetic and evolutionary relationships in selected pinus species using *rbcL* and *matK* chloroplast genes. *Open Journal of Plant Science*, vol. 6, no. 1, pp. 64-68. http://dx.doi.org/10.17352/ojps.000035.

SMITH, D.R., BURKI, F., YAMADA, T., GRIMWOOD, J., GRIGORIEV, I.V., VAN ETTEN, J.L. and KEELING, P.J., 2011. The GC-rich mitochondrial and plastid genomes of the green alga Coccomyxagive insight into the evolution of organelle DNA nucleotide landscape. *PLoS One*, vol. 6, no. 8, p. e23624. http://dx.doi.org/10.1371/journal.pone.0023624. PMid:21887287.

SOETAERT, S.S., VAN NESTE, C.M., VANDEWOESTYNE, M.L., HEAD, S.R., GOOSSENS, A., VAN NIEUWERBURGH, F.C. and DEFORCE, D.L., 2013. Differential transcriptome analysis of glandular and filamentous trichomes in *Artemisia annua*. *BMC Plant Biology*, vol. 13, no. 1, p. 220. http://dx.doi.org/10.1186/1471-2229-13-220. PMid:24359620.

STEVANUS and PHARMAWATI, M., 2021. Biodiversity and phylogenetic analyses using DNA barcoding *rbcL* gene of seagrass from Sekotong, West Lombok, Indonesia. *Biodiversitas*, vol. 22, no. 1, pp. 50-57. http://dx.doi.org/10.13057/biodiv/d220107.

SUSETYARINI, E., WAHYONO, P., LATIFA, R. and NURROHMAN, E., 2020. The identification of morphological and anatomical structures of *Pluchea indica*. *Journal of Physics: Conference Series*, vol. 1539, no. 1, p. 012001. http://dx.doi.org/10.1088/1742-6596/1539/1/012001.

TALLEI, T.E. and KOLONDAM, B.J., 2015. DNA barcoding of sangihe nutmeg (*Myristica fragrans*) using matK gene. *Hayati Journal of Biosciences*, vol. 22, no. 1, pp. 41-47. http://dx.doi.org/10.4308/hjb.22.1.41.

TINDI, M., MAMANGKEY, N.G.F. and WULLUR, S., 2017. The DNA barcode and molecular phylogenetic analysis several Bivalve species from North Sulawesi Waters based on COI gene. *Junal Pesisir dan Laut Tropis*, vol. 1, no. 2, pp. 32-38. http://dx.doi.org/10.35800/jplt.5.2.2017.15050.

TORELLA, A., ZANOBIO, M., ZEULI, R., DEL VECCHIO BLANCO, F., SAVARESE, M., GIUGLIANO, T., GAROFALO, A., PILUSO, G., POLITANO, L. and NIGRO, V., 2020. The position of nonsense mutations can predict the phenotype severity: a survey on the DMD gene. *PLoS One*, vol. 15, no. 8, p. e0237803. http://dx.doi.org/10.1371/journal.pone.0237803. PMid:32813700.

TRIYANI, Y., NAFSI, N., YUNIARTI, L., SEKARWANA, N., SUTEDJA, E., GURNIDA, D.A., PARWATI, I. and ALISJAHBANA, B., 2016. Macrophage mannose receptor gene (MMR) specific primer design for polymerase chain reaction (PCR) and deoxyribo nucleic acid (DNA) sequencing. *Indonesian Journal of Clinical Pathology and Medical Laboratory*, vol. 22, no. 2, pp. 158-162. http://dx.doi.org/10.24293/ijcpml.v22i2.1120.

ULRICH-MERZENICH, G., ZEITLER, H., JOBST, D., PANEK, D., VETTER, H. and WAGNER, H., 2007. Application of the "-Omic-" technologies in phytomedicine. *Phytomedicine*, vol. 14, no. 1, pp. 70-82. http://dx.doi.org/10.1016/j.phymed.2006.11.011. PMid:17188482.

WAHEED, U., 2012. *Histotechniques laboratory techniques in histopathology: a handbook for medical technologist*. Mauritius: Lap Lambert Academic Publishing.

WESTON, L.A., BARNEY, J.N. and DITOMMASO, A., 2005. A review of the biology and ecology of three invasive perennials in New York State: Japanese knotweed (*Polygonum cuspidatum*), mugwort (*Artemisia vulgaris*), and pale swallow-wort (*Vincetoxicum rossicum*). *Plant and Soil*, vol. 277, no. 1-2, pp. 53-69. http://dx.doi.org/10.1007/s11104-005-3102-x.

WIART, C., 2003. *Medicinal plants in Asia and Pacific for parasitic infections: botany, ethnopharmacology, molecular basis, and future prospect*. London: Elsevier.

WU, T., WANG, Y. and GUO, D., 2012. Investigation of glandular trichome proteins in *Artemisia annua* L. using comparative proteomics. *PLoS One*, vol. 7, no. 8, p. e41822. http://dx.doi.org/10.1371/journal.pone.0041822. PMid:22905110.

YANG, C.-H., WU, K.-C., CHUANG, L.-Y. and CHANG, H.-W., 2018. Decision tree algorithm generated single nucleotide polymorphism barcodes of *rbcL* genes for 38 Brassicaceae species tagging. *Evolutionary Bioinformatics Online*, vol. 14, pp. 1-9. http://dx.doi.org/10.1177/1176934318760856. PMid:29551885.

YUWONO, T., 2007. *Polymerase chain reaction theory and application*. Yogyakarta: Andi Publiser.

ZAGOTO, A.D.P. and VIOLITA, V., 2019. Leaf anatomical modification in drought of rice varieties (*Oryza sativa* L.). *Eksakta*, vol. 20, no. 2, pp. 42-52. http://dx.doi.org/10.24036/eksakta/vol20-iss2/201.

ZAREI, H., FAKHERI, B.A., NAGHAVI, M.R. and MAHDINEZHAD, N., 2020. Phylogenetic relationships on Iranian Allum species using the *matK* (cpDNA gene) region. *Journal of Plant Biotechnology*, vol. 47, no. 1, pp. 15-25. http://dx.doi.org/10.5010/JPB.2020.47.1.015.

ZHENG, S., KIM, H. and VERHAAK, R.G.W., 2014. Silent mutations make some noise. *Cell*, vol. 156, no. 6, pp. 1129-1131. http://dx.doi.org/10.1016/j.cell.2014.02.037. PMid:24630716.

ZUBAIR, Z., ISMATH, S. and SEYED, M.N.A., 2020. A comprehensive review with pharmacological potential of "mother of herbs" - *Artemisia vulgaris* Linn. *World Journal of Pharmacy and Pharmaceutical Sciences*, vol. 9, no. 8, pp. 240-251. http://dx.doi.org/10.20959/wjpps20208-16844.